Journal of Engineering and Technology for Industrial Applications

ITEGAM-JETIA

Manaus, v.11n.55, p. 59-72. September/October, 2025.
DOI: https://doi.org/10.5935/jetia.v11i55.1881

ISSN ONLINE: 2447-0228

RESEARCH ARTICLE OPEN ACCESS

IMPROVING THE EFFICIENCY OF THE TECHNOLOGICAL PROCESS OF ELECTROMECHANICAL TREATMENT OF MACHINE COMPONENTS BY MINIMIZING THE NUMBER OF CURRENT-CARRYING CIRCUIT ELEMENTS AND DESIGNING SPECIAL EQUIPMENT

Elena Veremey[1], Dmitriy Podashev[2]

[1,2] Kaliningrad State Technical University – Kaliningrad, Russia.

[1]http://orcid.org/0000-0001-7847-540X, [2]http://orcid.org/0000-0001-9112-9253

Email: elena.kerevichene@klgtu.ru , dmitrij.podashev@klgtu.ru

ARTICLE INFO

Article History
Received: April 17, 2025
Revised: May 20, 2025
Accepted: September 15, 2025
Published: September 30, 2025

Keywords:
electromechanical processing,
automated installation,
special equipment,
agricultural machinery parts,
energy saving

ABSTRACT

The article is devoted to improving the efficiency of the electromechanical processing technology for parts of agricultural machinery through minimizing the number of elements in the current-carrying circuit and designing special equipment. The authors examine the technology of electromechanical restoration and hardening of agricultural machinery components, focusing on the problems of spare parts shortage and insufficient production capacity of Russian manufacturers. Existing installations for electromechanical processing are analyzed, their advantages and disadvantages are identified, and the importance of automation processes for enhancing the performance characteristics of processed surfaces is emphasized. A developed prototype of an automated installation equipped with a specialized voltage analysis module and software that contributes to reducing electrical losses and improving equipment operating conditions is presented. The design features of the specially designed fixture are described, including calculations of key components and material requirements. Recommendations are provided regarding the selection of optimal designs and materials for creating various units of the fixture.

I. INTRODUCTION

Currently, the agricultural sector of the Russian Federation faces a significant shortage of tractors and other farm machinery [1]. At the same time, replenishing the fleet of combines and tractors in required volumes poses challenges because imports have been halted due to sanctions, while domestic producers cannot manufacture enough machines [1]. Given this situation, the qualitative indicators of Russia's agro-industrial complex will directly depend on both the quantity and quality of its agricultural machinery fleet in the near future [2]. Under these circumstances, it is essential to properly maintain and carefully operate existing equipment. Due to the lack of spare parts for foreign-made agricultural machinery and even domestically produced ones (it is known that up to 30...40% of components in domestic agricultural machinery consist of imported parts), there is a need to shift from component replacement to restorative and strengthening repairs [3-7].

There are numerous methods for treating and restoring parts, such as welding and overlay welding; galvanization and metallization; compression-plastic deformation; adhesion with plastics; application of polymeric materials onto worn surfaces, as well as electromechanical machining [4-21]. Electrochemical and electromechanical treatments have gained widespread use in hardening and restoring components of various mechanisms and machines, including those used in agriculture [7-10, 18, 19]. The essence of this type of part restoration lies in passing a high-current low-voltage electric current through a rolling tool. As a result, localized heating occurs in the contact zone between the roller and the part's surface, bringing metal into a plastic state. Through controlled heating and cooling of the contact area, highly durable and wear-resistant layers form on the surface, allowing not only restoration but also reinforcement of the parts.

Examples of electromechanical treatment aimed at restoring agricultural machinery parts are shown in Figure 1.

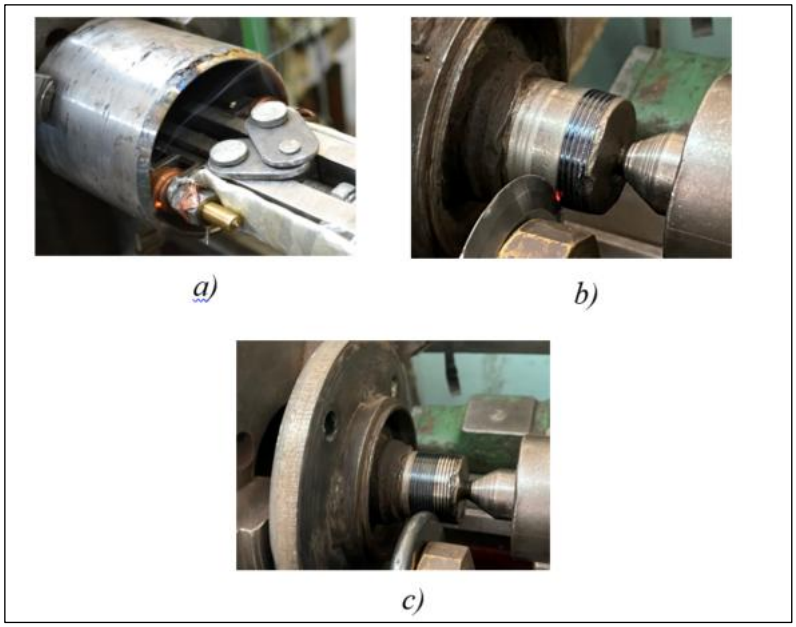

Figure 1: Examples of electromechanical treatment aimed at restoring agricultural machinery partsa: a) electromechanical hardening of the working surface of the vertical joint bushing of tractor K-701 and its modifications; b), c) restoration of the neck of the roller shaft axis of disk harrow BD-7 (b – electromechanical extrusion; c – electromechanical smoothing).
Source: Authors, (2025).

At present, the following types of installations for electromechanical processing are applied in Russian industry:

1. UEMO1 Installation – contains an autotransformer enabling stepwise adjustment of current intensity. Additionally, a rheostat provides smoother regulation within each step. Power supply voltage is 380 volts, rated power output is 10 kW, secondary winding delivers voltage ranging from 2 to 6 volts and current up to 1500 amperes. The unit is housed in an electrical cabinet, manual control is implemented. Due to intense heating during operation, liquid cooling of conductors is necessary, requiring access to a water source nearby. One drawback includes the heavy weight of the transformer, necessitating lifting equipment when moving the setup.
2. UEMO2 Installation – provides up to 1800 amperes in the secondary winding. It has rollers enabling mobility, otherwise similar to UEMO1.
3. Standard Installation – stationary power unit widely applicable, including as a current source for electromechanical processing. Unit weighs 120 kg. Its schematic arrangement does not differ significantly from previous models, delivering adjustable currents up to 3000 amperes.
4. Kasatka Installation – stationary device with manual control via switching transformer's stages and additional thyristor-based power regulation. Provides secondary winding currents from 0 to 5000 amperes, peak power rating is 25 kW. Liquid cooling of transformer and conductors is mandatory. Supply voltages can be either 380 or 220 volts.
5. EMUR Installation – compact transformer combined with a thyristor-controlled circuit. Allows connection of auxiliary management devices. Secondary winding outputs currents from 0 to 1500 amperes, maximum voltage is 4 volts. Unlike others, air cooling is employed instead of liquid cooling. Peak power consumption reaches 4 kW.

All reviewed installations feature manual controls except EMUR which lacks independent control means and requires additional connections. Continuous operator supervision is needed for all systems. Moreover, inconvenience, lengthy procedures, and inaccurate adjustments of power sources lead to subpar surface finish quality. Identified shortcomings provide sufficient grounds for developing a prototype capable of automating the process, increasing productivity and work quality, conserving electricity, and optimizing labor resources.

II. MATERIALS AND METHODS

The following research methods were used in preparing this article:

Theoretical methods.

Analysis of literary sources — studying and summarizing information from various publications dedicated to issues related to electromechanical processing and restoration of agricultural equipment parts.

Description of technologies and processes — detailed explanation of the essence of methods for restoring and hardening parts through electromechanical processing.

Review of installation designs — characterization of existing installations for electromechanical processing, identification of their advantages and disadvantages.

Experimental methods.

Conducting measurements — measuring electrical characteristics during operation of existing equipment, including voltage drop and energy loss in circuits.

Calculation of technical parameters — calculation of loads, stresses, and deformations of elements of special tooling designed for a new technological scheme.

Development of design solutions — creation of a new adaptive mounting system for transformers and design of frame components ensuring stability and reliability of the entire structure.

Creation of functional diagrams — development of a functional diagram of an automated installation incorporating a microprocessor controller and sensors that optimize the electromechanical processing procedure.

Engineering method.

Strength calculations — conducting engineering strength calculations for individual components of the tooling assembly, determining optimal cross-section sizes of steel profiles and diameters of metal shafts used in the framework and mechanism for moving carriages.

Using these methods allowed the authors to justify the need for developing specialized tooling, which contributes to increasing efficiency and accuracy of electromechanical part restoration while reducing energy losses and ensuring safe operation of the equipment.

III. RESULTS AND DISCUSSIONS

III.1. IMPROVING THE QUALITY OF ELECTROMECHANICAL PROCESSING USING A DEVELOPED ADAPTIVE SYSTEM FOR CONTROLLING TECHNOLOGICAL CURRENT

The basis for improving the productivity of the processing operation and enhancing its quality is the automatic control of the power supply unit with the option to switch to manual mode if necessary. This makes it possible to use more compact specialized units. Therefore, it is reasonable to automate the described process by utilizing software and a microcontroller, to which a measurement device will be connected during the operation of the installation. As a result, different operating algorithms can be set without altering the initial circuit or employing larger-sized equipment.

The functional diagram of this installation is shown in Figure 2.

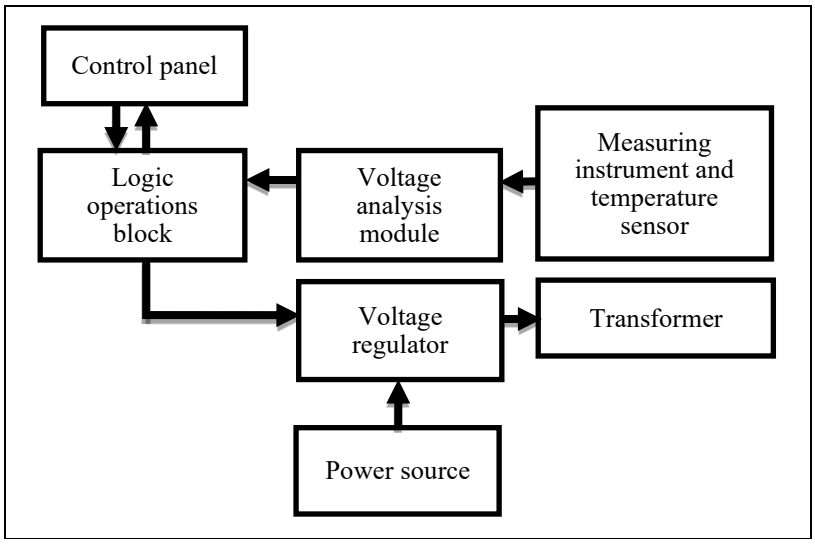

Figure 2: Functional diagram of the installation.
Source: Authors, (2025).

On the control panel are located the installation's controls such as: main toggle switch, mode selection toggle switch, current setting buttons, start button, and display for showing digital value of the current force. With the help of the control panel, the working mode of the installation and the current intensity are defined.

The logic operations block is intended for collecting and processing data, as well as sending commands to controlled devices according to the embedded program.

A measuring device is required to measure the contact resistance between the processing tool and the workpiece. It consists of an inductance coil wrapped around one of the conductors leading from the transformer to the tool. The current flowing along the conductor induces an induced current within the coil.

A temperature sensor is needed to monitor the temperature and prevent overheating of the processed surface.

The voltage analysis module converts the induced voltage in the coil into a digital format and sends it to the logic operations block.

The voltage regulator increases or decreases the electricity supply to the transformer based on commands received from the logic operations block.

Directly, the transformer converts standard network voltage into a voltage with specific characteristics suitable for implementing the technological process.

Additionally, there are five contacts available on the logic operations block for connecting a programmer to change the controlling program, as well as unused contacts that could be utilized for additional sensors.

It is proposed to use the Arduino Uno R3 model microcontroller, whose core is the ATmega8U2 chip.

Since the electric power source is quite compact (dimensions 115 × 150 × 275 mm), it is feasible to mount it directly onto the lathe saddle (model 1K62). This solution allows freeing up workspace from wiring cables and cooling hoses, thus reducing electromagnetic interference due to reduced cable length. An analysis was conducted regarding ways to secure the transformer, revealing no precedents for such type of mounting. Thus, designing a mounting construction becomes essential. Initially, the transformer was designed for spot-

welding applications where suspension-mounted equipment is commonplace, making the transformer's design adaptable to shocks and jolts during operation. Numerous fastening holes provide flexibility when choosing the attachment configuration.

III.2. DEVELOPMENT OF MOUNTING CONCEPT

To implement the above requirements, a mounting concept (Figure 3) has been developed using the Kompas-3D v.23 software package. This concept involves installing the power source on a carriage (Figure 4), which itself is mounted on guide rails providing single-degree-of-freedom movement (forward and backward) of the equipment.

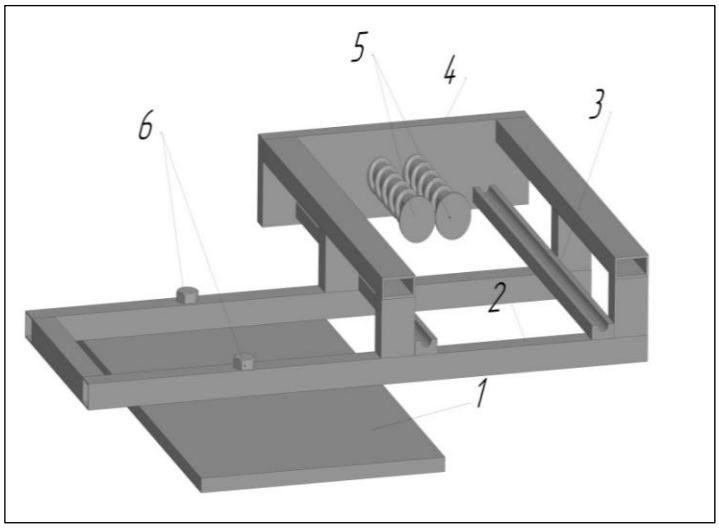

Figure 3: 3D model of adapter:
1 – Lathe saddle; 2 – Mounting adapter; 3 – Guide skids;
4 – Limit stopper; 5 – Spring damper; 6 – Fastening bolts
Source: Authors, (2025).

In order to avoid blocking the adjustment mechanisms of the lathe table-saddle stroke, it is necessary to shift the direction away from the center and perform appropriate strength calculations.

Furthermore, it has been suggested to replace some profile tubes with solid metallic elements of the same cross-section. Consequently, there arose a necessity to enhance the rigidity of the support node in order to adapt it for clinching and smoothing operations.

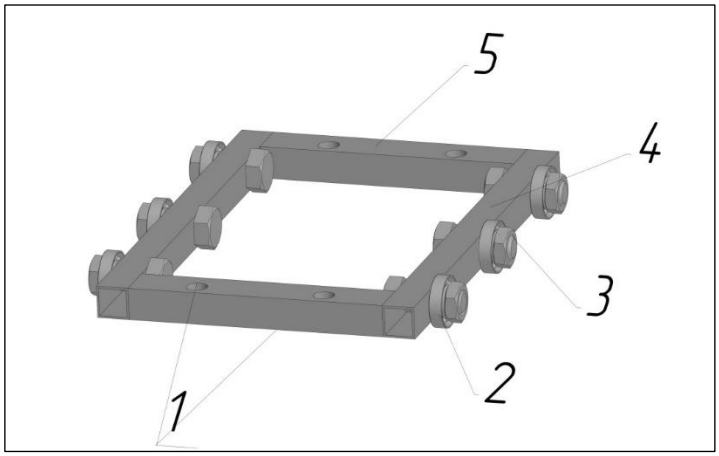

Figure 4: 3D model of carriage:
1 – Mounting holes; 2 – Bearings; 3 – Shaft; 4 – Support beam; 5 – Thrust beam (for springs of the main frame),
Source: Authors, (2025).

III.3. STRENGTH CALCULATIONS OF THE MAIN STRUCTURAL ELEMENTS

In analyzing the designed structure, certain difficulties arise due to the large number of components involved. Therefore, it was decided to divide this construction into separate components, replacing inter-component interaction connections with equivalent forces, followed by calculating each element individually.

Allowable loads on a specific area of known cross-section can be obtained using appropriate reference data.

During the design of the skids, it has been established that because of the large dimensions of equipment and workpiece, part of the skids will extend beyond the boundaries of the fastening table of the machine tool saddle (model 1K62). Consequently, it is necessary to select the section size and material for the skids which would meet strength requirements. It is essential to prevent deflection of the skids

under gravitational force. Based on these considerations, it was decided to use carbon structural steel grade 20 with a square cross-section measuring 20x20 mm.

Since part of the skids are rigidly fixed to the saddle table, any load applied at any point along them will be compensated by the reaction force from the support, limiting the strength of the product in this segment only by the strength of the material itself. The total calculated mass of the equipment amounts to 30 kg (~300 N).

The load on the skids appears as distributed since the carriage distributes the weight of the equipment across all six supports (see Figure 4). However, calculations should proceed based on worst-case loading conditions—when the entire weight of the equipment falls onto the portion of the skids located outside the support. In reality, however, cartridge movement will be limited by springs, resulting in lower actual loads on the skids.

According to the scheme for solving statics problems, we determine that finding unknown reactions requires considering equilibrium of the beam. At point A (Figure 5), there is an immovably rigid connection imposed on the beam, given that this part lies on the support and is bolted together. Thus, it becomes possible to free the beam by substituting the actions of the connection with reactions (H_A, R_A, M_A).

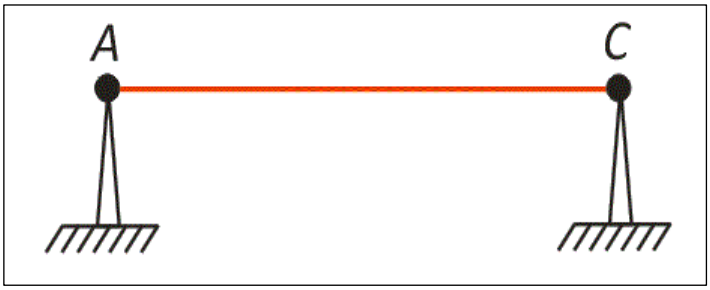

Figure 5: Horizontal weightless beam.
Source: Authors, (2025).

Support reactions are determined according to the beam equilibrium equation:

$$\sum F_x = 0, \sum F_y = 0, \sum M_A = 0.$$
$$\sum \mathrm{F_x} = 0: H_A = 0;$$
$$\sum F_X = 0 : R_A - q \times 160 = 0;$$
$$\sum M_A = 0 : M_A - q \times 160 \times (160 \div 2) = 0$$

Solving the obtained system of equations, we find the unknowns:

$$H_A = 0\ N;$$
$$R_A = q \pm 160 = 1{,}87 \times 160 = 300\ N;$$
$$M_A = q \times 160 \times (160 \div 2) = 1{,}87 \times 160 \times$$
$$\times (160 \div 2) = 23936\ N \times mm;$$

By formulating an additional moment equation relative to the free end of the beam, one can verify the performed calculations:

$$-160 \times R_A + M_A + q \times 160 \times (160 \div 2) = -160 \times 300 +$$
$$+ 23936 + 1{,}87 \times 160 \times (160 \div 2) = 0;$$

The transverse force is determined based on the following equation:

$$Q(X_1) = +R_A - q \times (X_1 - 0);$$

The value of Q at the edges of the section:

$$Q_1(0) = +300 - 1{,}87 \times (0 - 0) = 300\ N;$$
$$Q_1(160) = +300 - 1{,}87 \times (160 - 0) = 0\ N;$$

The bending moment is determined by the formula:

$$M(X_1) = +R_A(X_1) - M_A - Q_1 \times \frac{(X_1)^2}{2};$$

Thus, the values of the bending moments arising in the cross sections of the beam at the edges of the section are equal to:

$$M_1(0) = +300 \times 0 - 23936 - 1{,}87 \times \frac{(0-0)^2}{2} = -23936\ N \times mm;$$

$$M_1(160) = +300 \times (160) - 23936 - 1{,}87 \times \frac{(160-0)^2}{2} = 0\ N \times mm;$$

Based on the conducted calculations, it is possible to construct the stress diagram of the guideway (Figure 6).

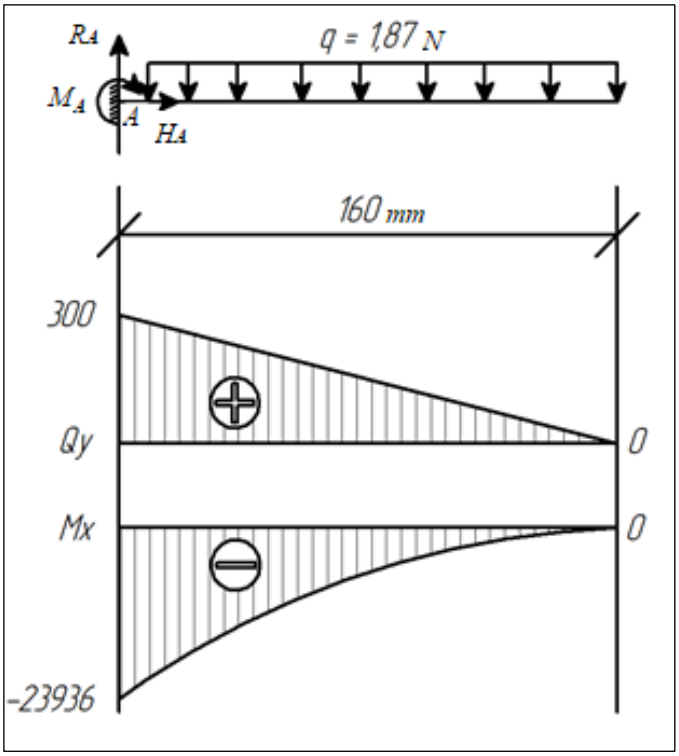

Figure 6: Load diagrams of guideway.
Source: Authors, (2025).

A rectangular beam cross-section is selected based on strength criteria with an allowable stress of 170 MPa, according to reference data.

$$\sigma = \frac{M_{MAX}}{W_X} \leq [\sigma],$$

where: σ – normal stresses, MPa; M_{MAX} – maximum absolute value of bending moment, determined from the M_X diagram, N·mm; W_X – section modulus, cm³; [σ] – permissible value of normal stress, MPa.

Thus, we obtain:

$$W_X = \frac{M_{MAX}}{[\sigma]} = \frac{23936}{170} = 140{,}8\ mm^3 = 0{,}141\ cm^3;$$

Since the width of the profile is known and equals 20 mm, the height of the profile can be determined using the formula:

$$h = \sqrt{\frac{6 \times W}{b}} = \sqrt{\frac{6 \times 0{,}141}{2}} = 0{,}649\ cm = 6{,}5\ mm$$

It should be noted that this value represents the minimum required to ensure the strength of the calculated beam, taking into account that there are two guide rails in the attachment structure. As a result, the weight of the equipment is evenly distributed, and also, considering that the used cross-section is much larger than the minimum calculated one, it can be concluded that the used structure meets the strength requirements.

Since the mounting adapter 2 (see Fig. 3) has an identical loading pattern to the guiding runners 3, a steel profile with a square cross-section of 20×20 mm will be adopted for its manufacture. This safety factor is necessary to enable the adapter to handle higher loads, particularly when attaching additional equipment or developing new operating modes.

Additionally, it is necessary to perform strength calculations for the shaft installed in the hole in the profile base of the carriage. Fastening occurs via nuts threaded on both sides, while a bearing is attached to the free end of the shaft. This arrangement allows the carriage to move along the guiding runners, with a total of six such axes provided on the carriage, three on each side. To achieve uniform distribution of the equipment's weight, the bearings must be mounted at regular intervals from each other and at the same height relative to the centerline of the profile in which they are secured, symmetrically positioned relative to the opposite side.

In this case, it is necessary to carry out a strength calculation for the axis. The load applied to it will cause bending, but this will be partially counteracted by the profile tube into which part of the axis is embedded. Despite these circumstances, let us calculate for the worst-case loading scenario for the axis: rigid fixation of one end and application of load to the other end, excluding details that hinder deformation of the axis from the loading scheme.

Shaft material: Steel 20, thread M12, length 28 mm.

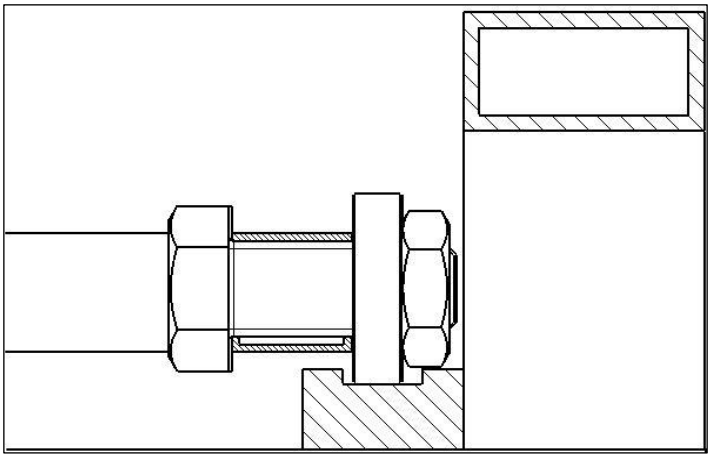

Figure 7: Bearing Mounting to Carriage.
Source: Authors, (2025).

Determination of support reactions according to the beam equilibrium equations:

$$\sum F_x = 0, \sum F_y = 0, \sum M_A = 0.$$
$$\sum F_x = 0: H_A = 0;$$
$$\sum F_X = 0 : R_A - P_1 = 0;$$
$$\sum M_A = 0 : M_A - 28 \times P_1 = 0;$$

Solving the obtained system of equations, we find the unknowns:

$$H_A = 0\ N;$$
$$R_A = P_1 = 50\ N;$$
$$M_A = 55 \times P_1 = 28 \times 50 = 1400\ N \times mm;$$

Let's check by forming an additional moment equation about the free end of the beam:

$$-28 \times R_A + M_A + 0 \times P_1 = -28 \times 50 + 1400 + 0 \times 50 = 0;$$

The stress diagram of the carriage shaft is shown in Figure 8.

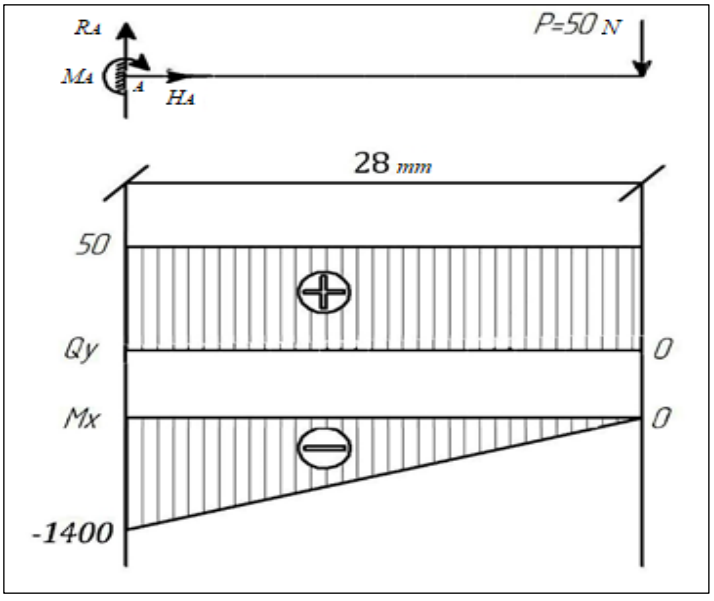

Figure 8: Stress diagrams of carriage shaft.
Source: Authors, (2025).

Transverse force Q:

$$Q(X_1) = +R_A;$$

Values of Q at the ends of the section:

$$Q_1(0) = +50 = 50\ N$$
$$Q_2(28) = +50 = 50\ N$$

Bending moment M:

$$M(X_1) = +R_A \times (X_1) - M_A;$$

Values of M at the ends of the section:

$$M_1(0) = +50 \times (0) - 1400 = 1400\ N \times mm;$$

$$M_2(28) = +50 \times (28) - 1400 = 0\ N \times mm;$$

Circular cross-section of the shaft is chosen based on strength conditions with an allowable stress $[\sigma] = 170\ MPa$.

Resistance moment of circular cross-section is defined by the formula:

$$W_X = \frac{\pi \times d^3}{32}$$

from where: $d = \sqrt[3]{\frac{32 \times W}{\pi} x}$

Required resistance moment:

$$W_X^{TP} = \frac{M_{MAX}}{[\sigma]} = \frac{1400}{170} = 0{,}008\ cm^3;$$

Thus, the diameter of the cross-section is determined as follows:

$$d = \sqrt[3]{\frac{32 \times W_X}{\pi}} = \sqrt[3]{\frac{32 \times 0{,}008}{3{,}14}} = 0{,}435\ cm = 4{,}4\ mm$$

This shaft diameter is minimally acceptable to provide sufficient strength. Considering the safety margin, it is reasonable to adopt a shaft diameter of 8 mm.

The stopper (see Fig. 3, position 4) serves to limit the travel of the carriage and install two springs on rods, which is necessary to create constant pressure on the carriage. The carriage, in turn, transmits pressure to the contact tool fixed on the transformer. Pressure adjustment is done through the traverse table feed lever. The total length of the springs in their uncompressed state should not exceed 100 mm, and the pressure exerted on the limiting stopper should not exceed 30 kg (or 300 N).

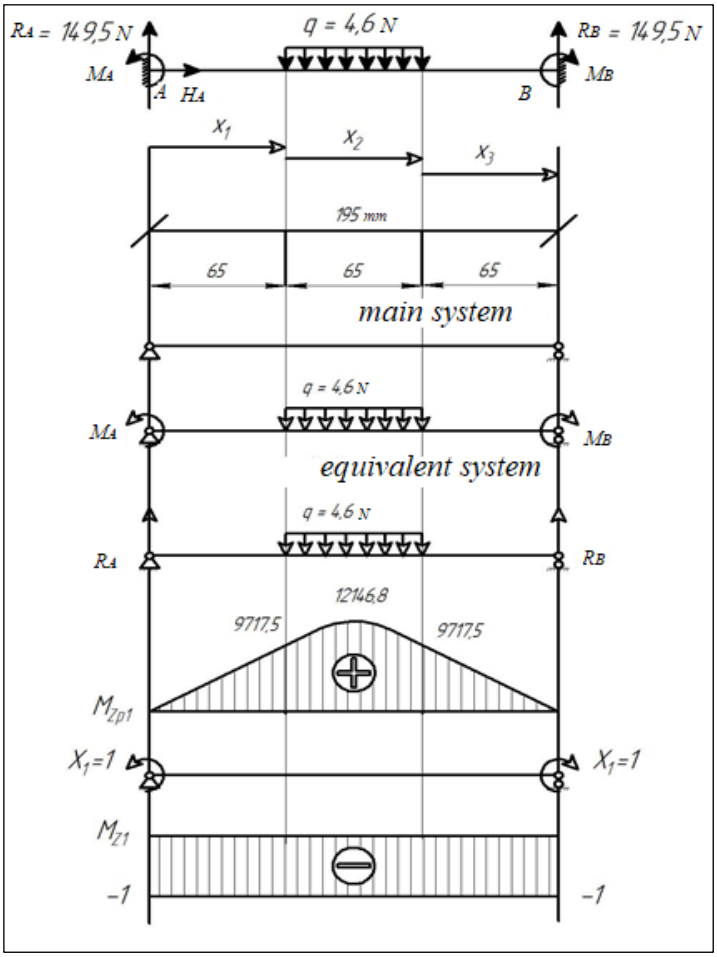

Figure 9: Main and equivalent loading systems of limit stop.
Source: Authors, (2025).

The system is statically indeterminate because the structure and load are symmetrical, so the force factors will also be symmetrical: $R_A=R_B$, $M_A=M_B$. To resolve the static indeterminacy, it is necessary to choose a primary system and compose the sum of projections of all forces onto the vertical axis:

$$\sum y = 0;$$
$$R_A + R_B - q = 0;$$
$$Q = 4{,}6\ N/mm \times 65 = 300\ \ N;$$
$$R_A = R_B = \frac{Q}{2} = 150\ \ N.$$

Then the equivalent system is: $\delta_{11} \times X_1 + \Delta_{1P} = 0$.

Constructing the canonical deformation equation, we build bending moment diagrams separately for external load q and separately for unit moments X_1=1.

From external loading, section 1: $(0 \le X \le 65)$:

$$Q_y = R_A = 149{,}5\ N;$$
$$M_Z = R_A \times X_1 = 149{,}5\ N;$$
$$for\ X_1 = 0; \quad M_Z = 0;$$
$$for\ X_1 = 65; \quad M_Z = 149{,}5 \times 65 = 9717{,}5\ N;$$

Section 2: $(0 \le X_2 \le 65)$:

$$Q_y = R_A - qX_2 = 149{,}5 \times X_2;$$
$$M_Z = R_A \times (64 + X_2) - \frac{qX_2^2}{2} = 149{,}5 \times X_2 - 2{,}3X_2^2 +$$
$$+ 9717{,}5\ \ N$$
$$for\ X_2 = 0;$$
$$Q_y = 149{,}5\ N;$$
$$M_Z = 9717{,}5\ N \times mm;$$
$$for\ X_2 = 32{,}5;$$
$$Q_y = 149{,}5 - 4{,}6 \times 32{,}5 = 0;$$
$$M_Z = 149{,}5 \times 32{,}5 - 2{,}3 \times 32{,}5^2 + 9717{,}5 = 12146{,}87\ N \times mm$$
$$for\ X_2 = 65;$$
$$Q_y = 149{,}5 - 4{,}6 \times 65 = -149{,}5\ N;$$
$$M_z = 149{,}5 \times 65 - 2{,}3 \times 65^2 + 9717{,}5 = 9717{,}5\ N \times mm.$$

Section 3: $(0 \le X_3 \le 65)$:

$$Q_y = -R_B = -149{,}5\ N;$$
$$M_Z = R_B \times X_3 = 149{,}5\ N;$$
$$for\ X_3 = 0; \quad M_Z = 0;$$
$$for\ X_3 = 65; \quad M_Z = 149{,}5 \times 65 = 9717{,}5\ N \times mm.$$

Canonical equation coefficients:

$$\delta_{11} = \frac{1}{EJ}\left[\int_0^{195}(-1)^2 dx\right] = \frac{195}{EJ};$$
$$\Delta_{1P} = \frac{1}{EJ}\left[2\int_0^{65}(149{,}5 \times X_1)(-1)dx_1 +\right.$$
$$\left. + \int_0^{65}(-2{,}3 \times X_2^2) + 149{,}5 \times X_2 + 9717{,}5)(-1)dx_2\right] =$$
$$= \frac{1}{EJ}\left[-149.5 \times 2 \times \frac{65^2}{2} + 2{,}3 \times\right.$$
$$\left. \times \frac{65^3}{3} - 149{,}5 \times \frac{65^2}{2} - 9717{,}5 \times 65\right] = \frac{-1368547{,}917}{EJ}$$

From the canonical deformation equation:

$$X_1 = -\frac{\Delta_{1P}}{\delta_{11}} = -\frac{-1368547{,}917}{195} = 7018{,}19\ N \times mm;$$

Thus, the system became statically determinate:

$$M_A = M_B = 7018{,}19\ N \times mm.$$

Final shear force (QY) and bending moment (MZ) diagrams in the equivalent system are presented in Figure 10.

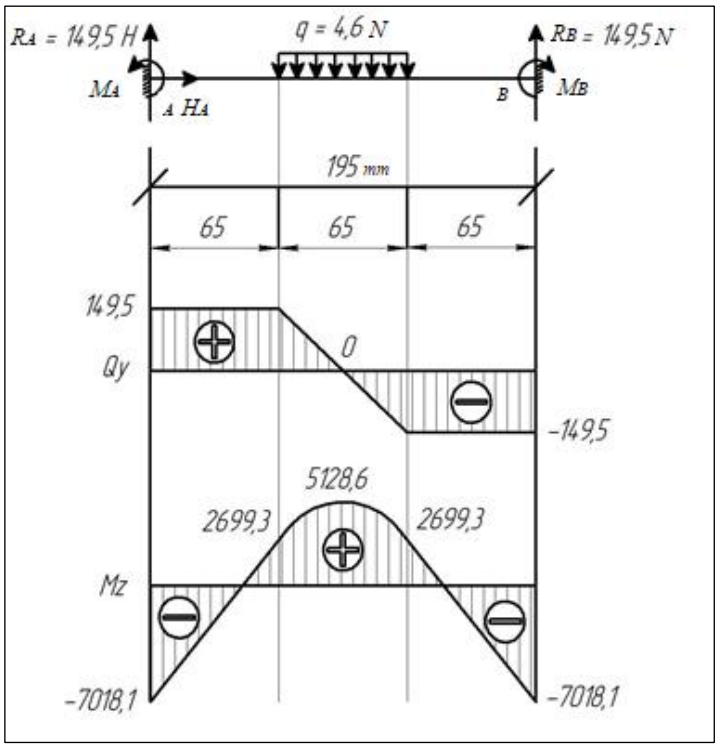

Figure 10: Final loading diagrams of limit stop.
Source: Authors, (2025).

Section 1: $(0 \le X \le 65)$:

$$M_Z = -M_A + R_A \times z_1 = -7018{,}19 + 149{,}5 \times z_1;$$
$$for\ z_1 = 0;$$
$$M_Z = -7018{,}19\ N \times mm;$$
$$for\ z_1 = 65;$$
$$M_Z = -7018{,}19 + 149{,}5 \times 65 = 2699{,}31\ N \times mm.$$

Section 2: $(0 \le X_2 \le 65)$:

$$M_Z = -M_A + R_A \times (65 + X_2) - \frac{qX_2^2}{2} =$$
$$= 2699{,}31 + 149{,}5 \times X_2 - 2{,}3X_2^2;$$
$$for\ X_2 = 0;$$
$$M_Z = 2699{,}31\ N \times mm;$$
$$for\ X_2 = 32{,}5;$$
$$M_Z = 2699{,}31 + 149{,}5 \times 32{,}5 - 2{,}3 \times 32{,}5^2 =$$
$$= 5128{,}69\ N \times mm.$$
$$for\ X_2 = 65;$$
$$M_Z = 2699{,}3 + 149{,}5 \times 65 -$$
$$-2{,}3 \times 65 = 2699{,}3\ N \times mm.$$

Section 3 is symmetrical to Section 1.
From the bending moment diagram M, it is determined that M_{MAX}=7018.1 $N{\cdot}mm$.

From the shear force diagram Q, Q_{MAX}=149.5 H.

Strength condition for bending based on normal stresses:

$$\sigma_{MAX} = \frac{M_{MAX}}{W_X} \leq [\sigma];$$

$$W_X = \frac{M_{MAX}}{[\sigma]} = \frac{7018{,}1}{160} = 0{,}044\ cm^3;$$

It follows that:

$$h = \sqrt{\frac{6 \times W}{b}} = \sqrt{\frac{6 \times 0{,}044}{2}} = 0{,}36\ cm = 3{,}6\ mm.$$

The minimum solid cross-section thickness required to ensure the structural strength is 20 x 3.5 mm. The project cross-section of 15 x 20 mm provides multiple times the strength reserve.

The tool depicted in Figure 11 is intended directly for contacting the surface of the processed part, specifically the roller axis of the contact tool.

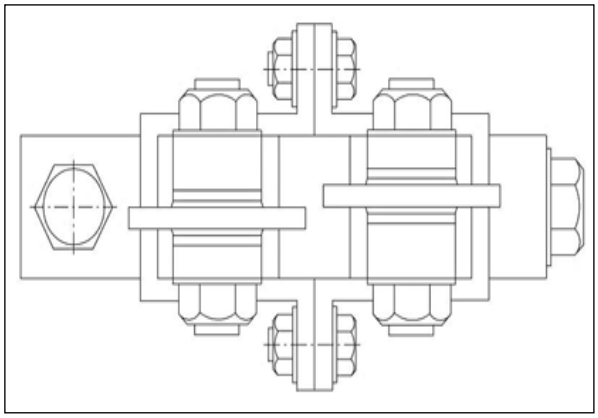

Figure 11: Contact Tool Scheme.
Source: Authors, (2025).

An electric current passes through this tool, heating the part as it travels through it, thereby implementing the process of electromechanical machining.

Material of the shaft: Steel 45, Length: 20 mm. It is necessary to calculate the load and select the cross-section.

According to the solution scheme for static tasks, to find unknown reactions, it is necessary to consider the equilibrium of the beam.

$$\sum F_X = 0: \quad H_A = 0;$$

$$\sum M_A = 0: \quad -q_1 \times 12 \times \left(\frac{12}{2}\right) + R_B \times 12 = 0;$$

$$\sum M_B = 0: \quad -R_a \times 12 + q_1 \times 12 \times \left(12 - \frac{12}{2}\right) = 0$$

Solving the obtained system of equations, we get: $H_A = 0\ N$.

Reaction of the hinged-moving support at point B:

$$R_B = \frac{\left(q_1 \times 12 \times \left(\frac{12}{2}\right)\right)}{12} = \frac{\left(25 \times 12 \times \left(\frac{12}{2}\right)\right)}{12} = 150\ N.$$

Reaction of the hinged-moving support at point A:

$$R_A = \frac{\left(q_1 \times 12 \times \left(12 - \frac{12}{2}\right)\right)}{12} = \frac{\left(25 \times 12 \times \left(12 - \frac{12}{2}\right)\right)}{12} = 150\ N.$$

We will perform verification:

$$\sum F_y = 0: \quad R_A - q_1 \times 12 + R_B = 150 - 25 \times 12 + 150 = 0.$$

Shear Force Q:

$$Q(X_1) = +R_a - q_1 \times (X_1 - 0);$$

Value of Q at the edges of the section:

$$Q_1(0) = +150 - 25 \times (0 - 0) = 150\ N;$$
$$Q_1(12) = +150 - 25 \times (12 - 0) = -150\ N.$$

Bending moment M:

$$M(X_1) = +R_a \times (X_1) - q_1 \times \frac{(X_1)^2}{2}$$

Values of M at the edges of the section:

$$M_1(0) = +150 \times (0) - 25 \times \frac{(0-0)^2}{2} = 0\ N \times mm;$$
$$M_1(12) = +150 \times (12) - 25 \times \frac{(12-0)^2}{2} = 0\ N \times mm.$$

Local extremum at point X=6:

$$M_1(6) = +150 \times (6) - 25 \times \frac{(6-0)^2}{2} = 450\ N \times mm.$$

Round cross-section is selected based on strength conditions with allowable stress:

$$[\sigma] = 170\ MPa;$$

Resistance moment of round cross-section is determined by the formula:

$$W_X = \frac{\pi \times d^3}{32},$$

it follows that:

$$d = \sqrt[3]{\frac{32 \times W}{\pi}} x.$$

The required resistance moment is determined by the formula:

$$W_X^{TP} = \frac{M_{MAX}}{[\sigma]} = \frac{450}{170} = 0{,}002\ cm^3.$$

Thus, the diameter of the cross-section is:

$$d = \sqrt[3]{\frac{32 \times W_X}{\pi}} = \sqrt[3]{\frac{32 \times 0{,}002}{3{,}14}} = 0{,}273\ cm = 2{,}7\ mm.$$

Loading diagrams of the roller in the contact tool are shown in Figure 12.

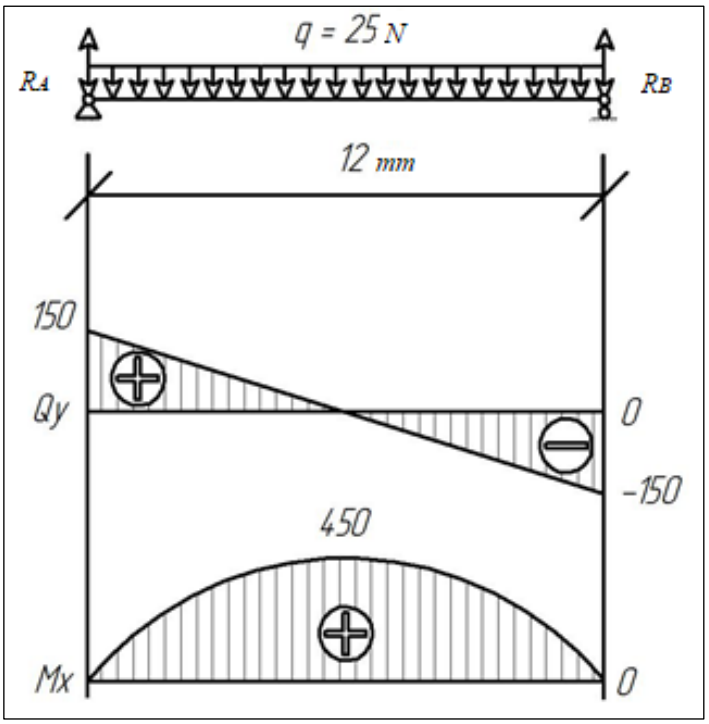

Figure 12: Roller loading diagrams in contact tool.
Source: Authors, (2025).

This shaft diameter is minimally acceptable to ensure sufficient strength. Taking into account the safety margin, we accept the shaft diameter of 10 mm.

IV. CONCLUSIONS

As a result of the research carried out, the technology of electro-mechanical treatment and its application area in strengthening and repairing agricultural machinery parts have been examined. It has been found that due to the shortage of spare parts for russian and foreign agricultural machinery, it is necessary to transition from modular replacement of parts and units to restorative and hardening repairs.

An analysis of existing installations for electro-mechanical processing has been conducted, noting their advantages and disadvantages. It has been revealed that a decrease in electrical current leads to uneven heating of the surface layer of parts, negatively affecting their strength characteristics.

Measurements taken during electro-mechanical processing showed a voltage drop in the power supply circuit from the current source to the tool-part contact, amounting to 27–36% of the initial level, with up to 50% of losses occurring in the current-carrying busbar. To reduce losses and improve technological efficiency, a conceptual schematic for electro-mechanical processing has been proposed, involving the use of a minimal number of elements in the power supply circuit.

Special equipment has been developed to implement the proposed electro-mechanical processing scheme, and strength calculations have been made for its major components. The proposed compact fixture, allowing for fewer electrical wires, reduces energy loss, improves occupational safety conditions, and enhances the effectiveness of the electro-mechanical processing technology for agricultural machinery parts.

V. AUTHOR'S CONTRIBUTION

Conceptualization: E. Veremey, D. Podashev.
Methodology: E. Veremey, D. Podashev.
Investigation: E. Veremey.
Discussion of results: E. Veremey, D. Podashev.
Writing: D. Podashev.
Review and Editing: E. Veremey, D. Podashev.
Resources: E. Veremey, D. Podashev.
Supervision: E. Veremey, D. Podashev.
Approval of the final text: E. Veremey, D. Podashev.

VI. REFERENCES

[1] N.I. Konyaeva, N.V. Konyaev T, "Features of Agricultural Machinery Repair in Modern Conditions", Modern Materials, Equipment and Technologies, no. 6 (45), pp. 125-130, 2022 (In Russian).

[2] A.V. Makarova, S.A. Grashkov, D.I. Es'kov, "The State of Domestic Agricultural Engineering and Ways to Increase the Efficiency of Agricultural Business", In the conference paper: Current Problems and Development Directions of Agroengineering in Russia, collection of scientific articles of the International Scientific and Technical Conference, Kursk, pp. 59-63, 2021 (In Russian).

[3] I.O. Ishkov, N.V. Konyaev, B.S. Blinkov, "Methods for Restoring Worn Parts", In the conference paper: Future of Science – 2022, Collection of Scientific Articles of the 10th International Youth Scientific Conference, Kursk, pp. 467-469, 2022 (In Russian).

[4] S.I. Zhdanov, N.V. Konyaev, "New Developments in Technology for Restoration and Hardening of Components", In the conference paper: Topical Issues of Innovative Development of Agroindustrial Complex, Proceedings of the International Scientific-Practical Conference, Publication Manager I.Ya. Pigorev, pp. 190-192, 2016 (In Russian).

[5] Yu.G. Alekhin, S.A. Grashkov, A.S. Ugrimov, "Quality of Welded Coatings on Plough Shares", In the conference paper: Quality in Production and Socio-Economic Systems, Collection of Scientific Papers of the 5th International Scientific and Technical Conference, Responsible Editor E.V. Pavlov, pp. 11-13, 2017 (In Russian).

[6] N.A. Pivovar, S.A. Grashkov, "Recovery of worn machine parts by plasma spraying of powders", In the conference paper: Actual problems of engineering and technical support of agro-industrial complex, Proceedings of the International Scientific and Practical Conference, pp. 22-29, 2013 (In Russian).

[7] E.V. Sazonov, M.E. Kulikov, S.A. Grashkov, "Restoration of Wear Resistance of Deep Loosener Working Elements", In the conference paper: Electric Power Today and Tomorrow, Collection of Scientific Articles of the International Scientific and Technical Conference, Kursk, pp. 147-153, 2022 (In Russian).

[8] S. Markauskas, "Investigation of surface electromechanical restoration process and it's quality", Transport Means, Proceedings of the International Conference, Kaunas, pp. 157-160, 2013.

[9] A. Shohiyon, Z. Obidov, "Restoration of the external surfaces of machine mechanisms by electromechanical treatment", Universum: technical sciences, no. 1-4(106), pp. 43-46, 2023.

[10] S.A. Yakovlev, M.M. Zamal'dinov, Y.V. Nuretdinova [et al.], "Electromechanical Hardening of VT22 Titanium Alloy in Screw-Cutting Lathes", Russian Engineering Research, no. 38, pp. 488-490, 2018.

[11] L. M. Jiang, W. Li, A. Attia [et al.], "A potential method for electrochemical micromachining of titanium alloy Ti6Al4V", Journal of Applied Electrochemistry, vol. 38, no. 6, pp. 785-791, 2008.

[12] N. Levov, A. Uhalin, "Innovations in restoration technology of automotive case details using adhesive method", Perspectives of Innovations, Economics and Business, vol. 4, no. 1, pp. 113-117, 2010.

[13] A.P. Chernysh, "Working out of information models of technological repair blocks for restoration of agricultural machine details", Traktori i Pogonske Mašine, vol. 17, no. 1, pp. 60-62, 2012.

[14] S. Y. Zhachkin, S. N. Sharifullin, N. A. Penkov [et al.], “About Modeling Kinematic Parameters of Deposition from Composite Electrochemical Coatings for Restoration of Details for Agricultural Machines”, IOP Conference Series: Materials Science and Engineering, vol. 570, p. 012104, 2019.

[15] V. Aulin, S. Lysenko, A. Hrinkiv [et al.], “Creation of theoretical bases of tribotechnologies of running-in and restoration as means of effective increase of operational wear resistance of motor transport and mobile agricultural machinery”, Problems of Tribology, vol. 99, no. 1, pp. 51-58, 2021.

[16] M. Denysenko, “Restoration and Strengthening of Parts and Tool of Agricultural Machinery Operating in an Abrasive Environment”, National Interagency Scientific and Technical Collection of Works. Design, Production and Exploitation of Agricultural Machines, no. 53, pp. 271-284, 2023.

[17] N. Wu, Q. Wang, “Repair of vibrating delaminated beam structures using piezoelectric patches”, Smart Materials and Structures, vol. 19, no. 3, p. 035027, 2010.

[18] P.A. Boykov, A.S. Bezruk, Y.I. Melnikov [et al.], “Repair and restoration of critical components of timber harvesting machines using electromechanical processing”, Systems. Methods. Technologies, no. 4(60), pp. 38-42, 2023 (In Russian).

[19] R. Bini, M. Monno, M. I. Boulos, “Effect of Cathode Nozzle Geometry and Process Parameters on the Energy Distribution for an Argon Transferred Arc”, Plasma Chemistry and Plasma Processing, vol. 27, no. 4, pp. 359-380, 2007.

[20] R. Hamano, H.R. Costa, T. Chuvas, “Evaluation of Machining Forces and Surface Integrity on AISI 304 Steel Top Milling Process under Different Cutting Conditions”, Itegam-Jetia, no. 5(20), pp. 166-171, 2019.

[21] S. Doshi, K. Vaghosi, N. Mehta, “Progress in the welding of AL alloy thin sheet and future prospectus for automobile”, Itegam-Jetia, no. 10(46), pp. 42-49, 2024.